Immunity, Vol. 23, 309–318, September, 2005, Copyright ©2005 by Elsevier Inc. DOI 10.1016/j.immuni.2005.08.009

Functional Connectivity between Immune Cells Mediated by Tunneling Nanotubules

Simon C. Watkins[1,2] and Russell D. Salter[2,*]
[1]Department of Cell Biology and Physiology
[2]Department of Immunology
University of Pittsburgh School of Medicine
Pittsburgh, Pennsylvania 15213

Summary

Intercellular signals can be transmitted through neuronal synapses or through gap junctions, with the latter mediating transmission of calcium fluxes and small molecules between cells. We show here that a third form of communication between cells can be mediated by tunneling nanotubules (TNT). When myeloid-lineage dendritic cells and monocytes are triggered to flux calcium by chemical or mechanical stimulation, the signal can be propagated within seconds to other cells at distances hundreds of microns away via TNT. A complex and transient network of TNT is seen in live cells, with individual tubules exhibiting substantial variation in length and diameter. In addition to calcium fluxes, microinjected dye tracers can be transferred through these connections. Following TNT-mediated stimulation, spreading of lamellipodia occurs in dendritic cells characteristic of that seen during the phagocytic response to bacteria. These results demonstrate that nonneuronal cells can transmit signals to distant cells through a physically connected network.

Introduction

Many cellular responses are initiated by engagement of surface receptors. In dendritic cells (DC) and other myeloid lineage cells, toll-like receptors (TLR) play a critical role by binding microbial products or endogenous mediators of inflammation and initiating cell activation or maturation (Pasare and Medzhitov, 2004). Distinct TLR have been identified that bind individual compounds from bacteria, fungi, and viruses, and potentially also endogenous ligands such as heat shock protein 70 and gp96. Engagement of individual TLR on DC and macrophages stimulates well-defined intracellular signaling programs, with subsequent alterations in cell motility and vesicular trafficking, followed by induction of unique transcriptional programs (Agrawal et al., 2003; Bambou et al., 2004; Fitzgerald et al., 2004; Park et al., 2004; Takeda and Akira, 2004). These observations lead to a consensus model in which engagement of TLR receptors and downstream signaling events are crucial for proper functioning of antigen-presenting cells. Inherent in this model is the assumption that individual cells become activated solely through engagement of receptors on their own surfaces. This has not been directly demonstrated, however, since most assays of cellular activation measure changes in bulk properties within cultures rather than examining individual cells.

We recently used live-cell imaging to show that individual DC respond to exposure to *E. coli* by rapidly extending membrane veils, or lamellipodia, that can bind the bacteria and transport them along the plasma membrane to the central region of the cell where internalization occurs (Salter et al., 2004). In this system, cells were imaged continuously prior to and after introduction of medium containing bacteria. Direct contact with bacteria was not required for veil extension, and we concluded that exposure to soluble factors derived from the bacteria activated DC to increase the efficiency of antigen capture. Potentially related findings were reported using mouse bone marrow-derived DC, which lose podosome-mediated attachment to the substrate in response to LPS exposure, while simultaneously increasing their ability to uptake soluble ligands (West et al., 2004).

These results suggest that dendritic cells respond very rapidly (within seconds to minutes) upon exposure to bacterial products. To study this further, we refined our system so that stimuli could be delivered to individual cells with concurrent imaging. A glass microinjection tip was used to deliver ligands to cells labeled with fura-2, as a way to measure calcium fluxes indicative of one of the first steps of cellular activation. Our study demonstrates that myeloid cells rapidly respond to soluble mediators and to mechanical stimulation and unexpectedly can amplify this cellular activation response by intracellular signaling across large networks of cells, interconnected via patent tubular connections.

Results

Calcium Fluxes Are Induced in DC after Exposure to Bacterial Products

Cell-free bacterial supernatant was obtained from *E. coli* BL21 strain and tested for ability to stimulate calcium fluxes in human monocyte-derived DC. Individual colonies picked from agar plates were dispersed into tissue culture medium, and after 5 min cells were pelleted by centrifugation. The supernatant was collected and passed through a 0.2 μm syringe filter. This *E. coli* supernatant (ECS) was loaded into a glass microbore injection tip and positioned above cells grown on collagen-coated glass chamber slides. ECS was then released into the medium at a continuous slow rate (1 nl/min), which triggered calcium fluxes in many DC within the field, as shown in Figure 1A. This response was not evident in all cell types, and THP-1 monocytes did not show fluxes when similarly stimulated with ECS (see Figure S1 in the Supplemental Data available with this article online). In addition, not all DC within a given field responded, and some cells were observed to flux several times. The flux was not propagated evenly as a wave from the source of ECS, as might have been expected for stimulation by a diffusible soluble mediator. As a control, Cy3-labeled Fab fragments diluted into

*Correspondence: rds@pitt.edu

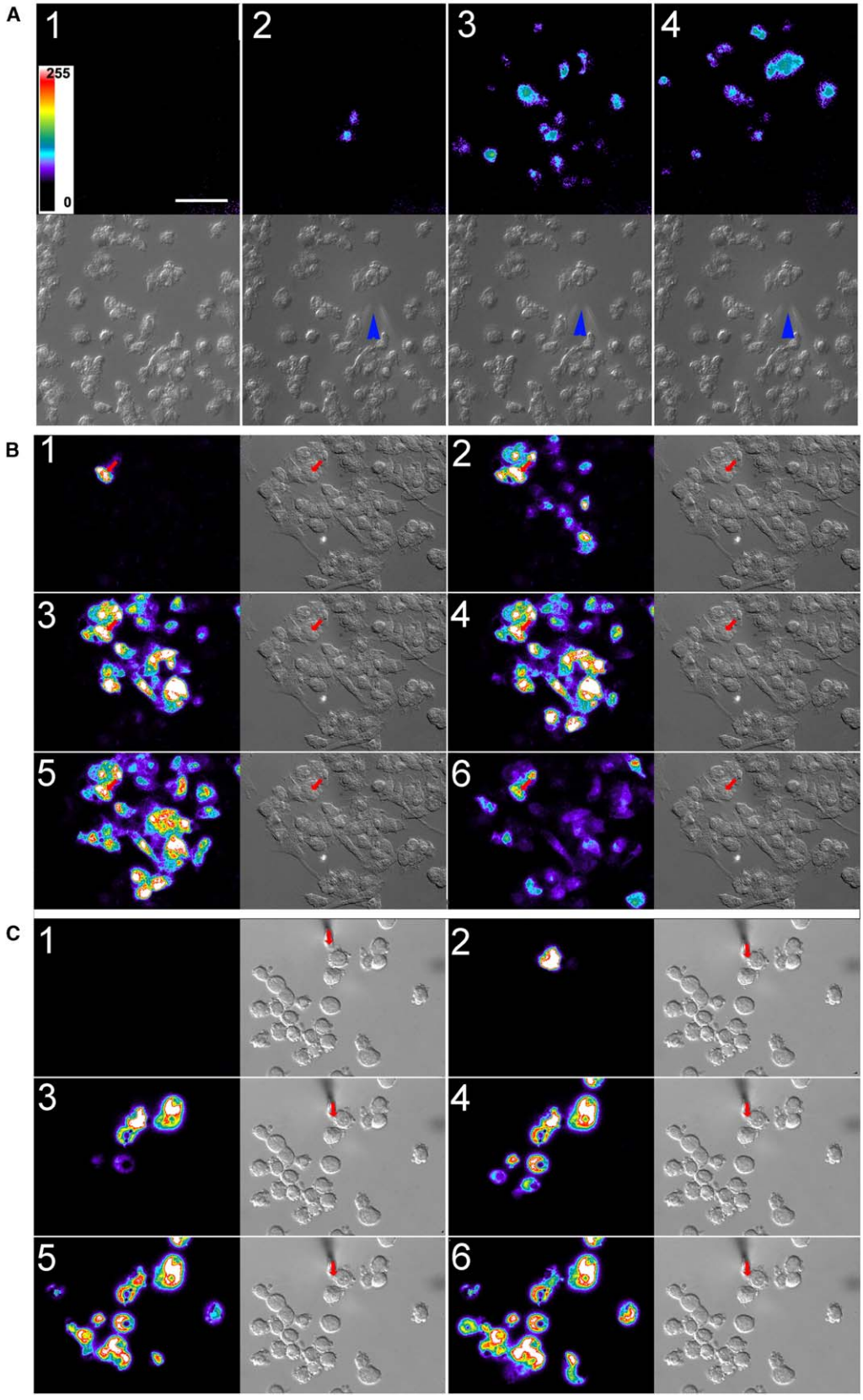
A
1
2
3
4
255
0
B
1
2
3
4
5
6
C
1
2
3
4
5
6

the same medium was released near cells, and this did not stimulate a calcium flux in multiple experiments (data not shown). This indicates that the medium itself is not stimulatory. Cy3-labeled Fab was thereafter routinely included as a tracer to confirm that the microinjection tip was patent during injection.

Mechanical Stimulation of Myeloid Cells Induces Calcium Fluxes that Are Propagated to Adjacent Cells in Culture

The calcium fluxes seen above cannot be readily explained by a gradient established via diffusion of the stimulatory mediator, since DC were observed to flux intermittently at distances up to 100 μm away from the injection source, while some cells nearer to the source did not respond. We hypothesized that DC might be physically connected through extended processes that could allow for cell-to-cell transmission of fluxes. To test this directly, we took advantage of the accidental observation that mechanical contact of a cell with the tip stimulated a calcium flux. Strikingly, we noted that the flux was propagated to other cells within the field, even when a fresh tip was used without any injection of material (Figure 1B, see also Movie S1). This supports the hypothesis that physical connections between DC in culture are present that can allow for propagation of signals from an originating cell to other cells.

We next examined whether transmission of calcium fluxes occurred in other cells types. Fibroblasts and HeLa cells that were stimulated mechanically responded individually, but there was no transmission to adjacent cells in culture (data not shown). THP-1 monocytes, however, also responded to contact stimulation and were able to transmit the flux throughout a field of adjacent cells (Figure 1C, see also Movie S2), although as shown in Figure S1, they were unresponsive to ECS. In both DC and THP-1 cells, this response was dependent upon extracellular calcium, as 0.5 mM EDTA effectively inhibited propagation (data not shown). Propagation from the point of stimulation was rapid, with an initial speed of 35 $\mu m\ s^{-1}$, which slowed rapidly to 10–15 $mm\ s^{-1}$ as shown in Figure S2. Transmission of flux could be observed up to 0.5 mm away from the point of stimulation in densely seeded fields (data not shown). These results demonstrate that transmission of calcium fluxes by myeloid lineage cells is robust.

It is evident that even following mechanical stimulation, not all cells within a field fluxed calcium (Figures 1B and 1C). This selectivity coupled with the rapidity of cell-to-cell transmission suggested that the response was not likely to result from release of diffusible mediators from damaged cells. To further address this issue, we identified a single cell within a multicell field that responded to mechanical probing by calcium fluxing in isolation (Figures S3A and S3B). After 30 s of inactivity (Figure S3C), another cell nearby was probed (Figure S3D), and this led rapidly to calcium fluxes in nearly all adjacent cells (Figures S3E–S3H, see also Movie S3). This supports the conclusion that mechanical probing and the resulting response visualized by calcium fluxing does not cause the release of soluble material into the surrounding medium that would be able to induce responses in adjacent cells.

Calcium Fluxes Triggered by Bacterial Supernatants Can Be Propagated to Adjacent Cells

It was important to determine directly whether propagation of calcium fluxes could occur after stimulation by an exogenous soluble stimulator such as ECS, since the physiologic relevance of mechanical stimulation in uncertain. To test this, we took advantage of the observation that THP-1 cells do not respond to ECS, but can be induced to propagate a signal initiated in other cells (Figure 1C). DC were cocultured with THP-1 cells for 1 day, before labeling with fura-2 and antibody against CD11c. The latter was used to distinguish marker-positive DC from marker-negative THP-1 cells. ECS was injected in the vicinity of cells with continuous imaging. As shown in Figure 2, DC responded to ECS, followed within seconds by fluxes in several adjacent THP-1 cells. This demonstrates that a soluble mediator can initiate a signal within a cell that is propagated to surrounding cells that are not themselves directly responsive to the soluble mediator.

Transmission of Calcium Fluxes Is Not Mediated by Gap Junctions or by Release of ATP from Stimulated Cells

It was recently reported that Langerhans cells in the skin express connexin 43 and that gap junctions permit passage of small molecules between cells (Neijssen et al., 2005). Since gap junctions transmit calcium fluxes in many cell types, we tested whether treatment with α-glycyrrhetinic acid, which inhibits gap junction func-

Figure 1. Propagation of Calcium Fluxes in Myeloid Cells Following Stimulation with *E. coli* Supernatants or Mechanical Stimulation

(A) Stimulation of calcium fluxes in dendritic cells. ECS was mixed with Cy3-Fab and loaded into a femto-tip that was placed into the microinjector. A field of cells was identified visually and the tip positioned directly above the cells before release of material. Each panel shows a pseudocolored intensity image for the calcium signal above the corresponding differential interference contrast image (see inset panel 1 for intensity values). The blue arrow indicates the position of the microinjection tip. No calcium signal (above background) was evident before ECS was delivered through the microinjection tip (panel 1). Flux occurs and spreads rapidly (panels 1–4 show 1 s intervals) after ECS is delivered.

(B) Mechanical stimulation induces calcium fluxes in dendritic cells. Each panel shows a pseudocolored intensity image for the calcium signal on the left and the corresponding differential interference contrast image on the right. The red arrow indicates the position of the microinjection needle used to touch the cell. Each frame (2–5) is separated by 2 s following stimulation in panel 1. Following a robust calcium flux in the stimulated cell (panel 1), the flux is seen to radiate out from this cell across the entire field of view. Panel 6 shows an image collected at 15 s; in this image it can be seen that the intracellular calcium levels are returning to baseline levels.

(C) Mechanical stimulation of THP-1 monocytes induces calcium fluxes. Experiment was performed as in (B) with 2 s intervals shown. Scale bar equals 50 μm in all panels (shown in panel 1 of [A]). Similar results have been observed in more than 50 independent experiments.

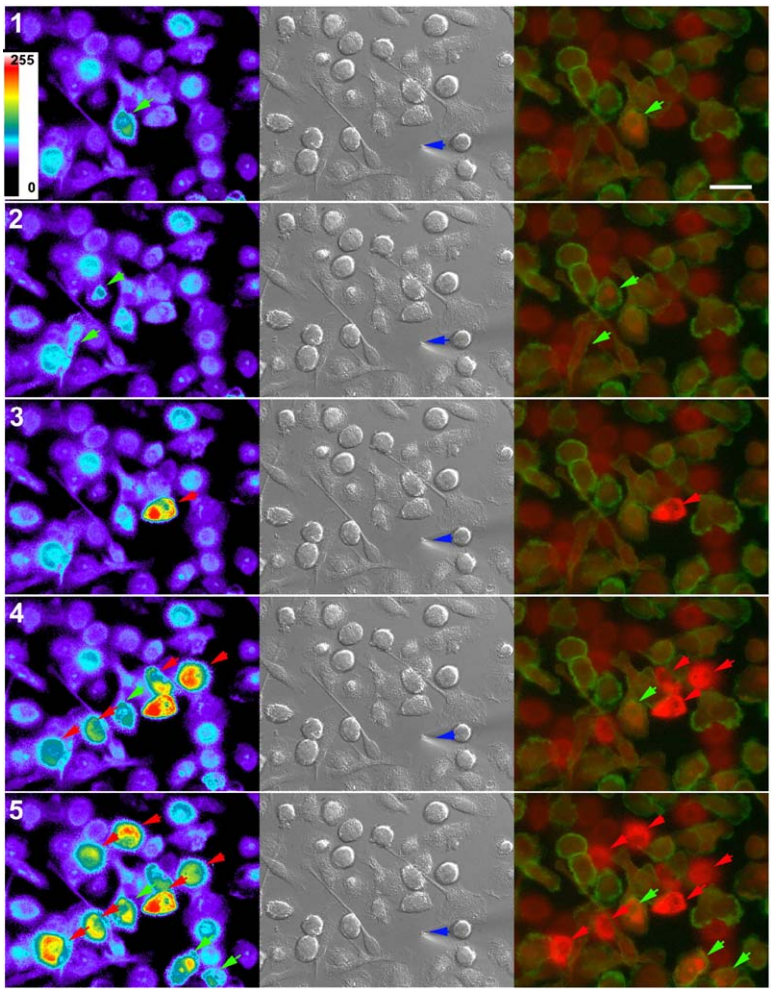

Figure 2. Propagation of Calcium Fluxes from DC to THP-1 Monocytes

ECS was released in the vicinity of a DC (identified by CD11c expression) in chamber slides in which DC and THP-1 cells were co-cultured. The injection tip is indicated by the blue arrows. Panels in the left column show pseudocolored intensity images for the calcium signal (see inset panel 1, left, for intensity values) following release of ECS. Panels in the middle column show the corresponding differential interference contrast images, and panels in the right column show the overlay of the calcium flux image (here false colored red) and CD11C (green), the latter to distinguish DC from THP-1 cells. A single DC (green arrow in panel 1, right) is seen to flux at the first time point, shortly after release of ECS. After 1 s, two other DC flux (green arrows in panel 2, right), followed 1 s later by flux in a THP-1 cell (red arrow in panel 3, right). Additional DC and THP-1 cells flux over the next 2 s (panels 4 and 5). It should be noted that variations in intensity are not readily observed in monochrome (red) images in the right column and are much more readily observed in the quantitative pseudocolored panels in the left column. Microinjection of Cy3-IgG is medium, which is used to confirm the tip is patent, did not induce calcium fluxes in either cell type (data not shown). Mechanical stimulation of either cell type resulted in fluxes that were propagated to the other cell type (data not shown). Scale bar equals 20 μm. Results are representative of four independent experiments.

tion, blocked calcium flux transmission. We did not observe inhibition of flux propagation following mechanical stimulation when THP-1 cells were pretreated with the drug at a concentration of 10 mM (data not shown). Higher concentrations proved toxic to cells. In addition, the highly specific gap junction inhibitor gap27, which is a peptide derived from connexin 43, was tested (Boitano and Evans, 2000). No inhibition of calcium flux transmission in THP-1 cells was observed at a concentration that blocked transfer of fluorescent compound Lucifer yellow between intestinal epithelial cells following microinjection (data not shown). This suggests that gap junctions are not responsible for flux transmission in the cell we have examined. This is further supported by the observation that fluxes can be propagated between myeloid cells that are not in close proximity, but are separated by up to 10–20 μm.

We also addressed whether ATP released from myeloid cells following mechanical stimulation could be responsible for propagating calcium fluxes, based on a previous report demonstrating such a mechanism in mast cells (Osipchuk and Cahalan, 1992). Addition of BzATP, a stabilized form of ATP, did not stimulate fluxes in THP-1 cells (data not shown). Likewise, responses induced in THP-1 cells by mechanical stimulation were not blocked by suramin (data not shown), an antagonist of P2 purinergic receptors responsible for ATP-mediated responses in mast cells. Oxidized ATP (o-ATP), which blocks purinergic receptor function by covalent attachment, similarly had no effect when cells were pretreated at a concentration of 0.5 mM for 2 hr before mechanical stimulation. Furthermore, it was reported that waves of calcium flux were transmitted at a rate of 5–10 μm s^{-1} in mast cells, which is somewhat slower than we observed in myeloid cells. These observations rule out the possibility of ATP-mediated propagation as an explanation for the current results.

Evidence of Direct Physical Connections between Myeloid Lineage Cells

Since all of the data above were consistent with physical connections between myeloid cells distinct from gap junctions, we next used high-resolution DIC imaging to examine groups of cells in culture. Fine tubular structures up to 100 μm in length were seen to connect THP-1 cells (Figure 3B). These appeared to match the previously reported description of tunneling nanotubules (TNT), which range in diameter from 50 to 200 nm (Rustom et al., 2004). Since this is below the diffraction-limited resolution of light microscopy, we used a fluorescently labeled antibody against class I MHC to better visualize TNT, based on a previous report that

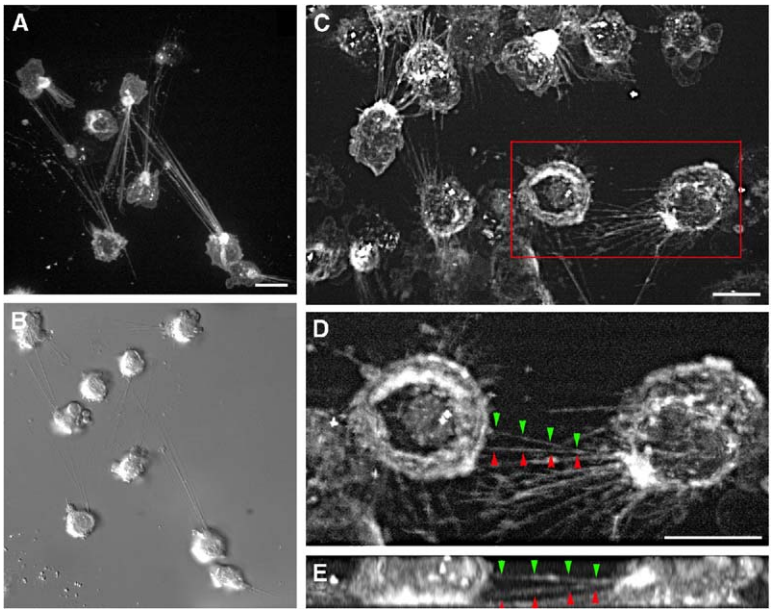

Figure 3. TNT Interconnect Live THP-1 Cells

(A and B) DIC (A) and a maximum intensity confocal projection of cells (B) following staining of live DC with anti-class I antibody (mouse anti-human HLA-A,B,C class I MHC; Alexa 488 conjugated, Serotec) shows extensive TNT running between cells in the field over distances in excess of 100 μm. Similar results were obtained with DC; however, fewer TNT and cell-to-cell connections were observed.

(C) A live-cell maximum intensity projection confocal image MHC class I staining of live THP-1 cells is shown. Extensive TNT connect cells throughout the field.

(D) An enlargement of the cells outlined in red in (C). Two TNT are highlighted, one with green arrows, the other with red arrows.

(E) An XZ projection of these two cells, demonstrating that the two highlighted TNT run above the surface of the substrate. Scale bar equals 15 μm. Results are representative of five independent experiments.

EGFP-tagged class I MHC molecules localize in these structures (Onfelt et al., 2004). The cells were then imaged using live-cell confocal methods followed by generation of a maximum intensity projection. This approach revealed many more TNT than we were able to observe with DIC analysis (Figure 3A, see also Movie S4), with great variability in length and number of connections observed between cells. Quantification showed that between 0 and 75 TNT may be present per cell, and these were more abundant in cells in close proximity. While TNT were most commonly seen to originate from and terminate on the lower portion of cell bodies, they were not confined to the substratum. This is seen in Figure 3D, which shows an enlarged part of Figure 3C with arrows (red and green) marking two individual TNT. Figure 3E also shows an XZ projection, demonstrating that these TNT are elevated above the substratum. This result might explain why reduced numbers of intact TNT are seen in fixed samples, as shown in Figure S4A, a low-power SEM image showing that connections that still exist between cells are primarily those at the dish surface. Figure S4B shows numerous discontinuous fragments of TNT that are in the vicinity of cells. A higher-magnification SEM image of a single representative thin TNT (average diameter 35 nm) is also shown. Confocal microscopy of fixed specimens shows a similar paucity of TNT and demonstrates the presence of actin within those that remain (Figure S4D; similar results were seen for class I MHC staining, data not shown). Thus, fixation and mechanical effects may destroy the majority of TNT. In live cells, individual connections are relatively transient. Live-cell time-lapse confocal microscopy shows that the connections form and disappear frequently between cells over a period of several minutes, as seen in Figure 4.

Transmission of Calcium Fluxes by TNT

If TNT are responsible for transmitting induced signals from cell to cell, we hypothesized that calcium fluxes originating from the stimulated cell and moving down TNT toward connected cells should be evident. This was in fact the case in DC as shown in Figure 5 (see also Movie S5), and it should be noted that reverse fluxes toward the stimulated cell were never observed. Only relatively large-diameter TNT were able to transmit calcium fluxes that were visible, perhaps due to difficulties in discerning signal above background for thinner TNT. It was also apparent that immediately following fluxing, large TNT underwent morphologic changes, appearing less rigid and attaining a beaded appearance (Figure 5, panels 5–6). In a previous report, it was suggested that beads visible within TNT represent endosomes, based on staining with lysotracker dye (Rustom et al., 2004). We consider this to be unlikely in the cells we have studied, since the beads appear evenly distributed throughout the structure almost immediately after the flux passes.

Calcium fluxes transmitted by a network of TNT should be blocked if the network were disrupted. We tested this by scraping a culture dish of THP-1 cells with a pipette tip, removing cells from a strip approximately 100 μm wide and, in addition, destroying TNT connections. If fluxes were transmitted by physical connections rather than by diffusible mediators, we predicted that mechanical stimulation of cells on one side of the strip should generate a flux transmitted only on that side, while a mechanism involving diffusible mediators should be able to propagate to both sides. As shown in Figure S5, mechanical stimulation of a single cell resulted in flux transmission that was limited to cells on that side of the culture. When a cell on the opposite side was stimulated, reciprocal results were obtained (data not shown).

Phenotypic Changes in DC Induced via TNT-Mediated Signaling

As we reported previously, DC extend lamellipodia in response to stimulation with bacterial products (Salter

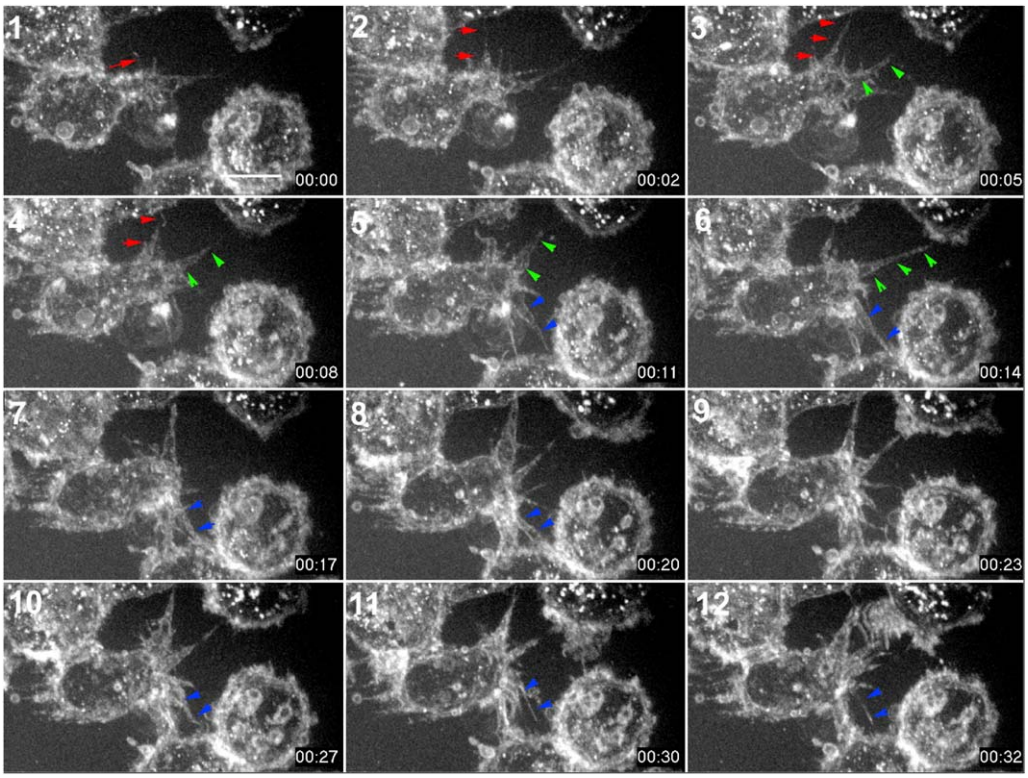

Figure 4. TNT Form and Alter Shape over Time

Each panel in this figure shows a single THP-1 cell forming tubular connections with other cells in the field and is a live-cell confocal maximum intensity projection in cells stained with antibody to class I MHC. Each set of colored arrows shows the development and regression or maintenance of individual TNT over time. Panels are separated by approximately 3 min, and indicated times are in minutes. Results are representative of five independent experiments. Scale bar equals 10 μm.

et al., 2004). Since spreading is one of the earliest responses seen in phagocytes following stimulation (Ballarin et al., 2002; Cox et al., 2002; Wells et al., 2004), we asked whether TNT-mediated signaling would induce this characteristic response in DC. As shown in Figure 6 (see also Figure S6 and Movie S6), spreading was observed in several DC within 1–2 min after calcium fluxing was induced by contact stimulation of an adjacent connected cell. In Figure 6, DC were labeled with anti-CD11c-allophycocyanin (APC) to accentuate veil extension in two cells that showed strong calcium fluxes following mechanical stimulation of a distant cell. A cell that did not flux calcium and does not show veil extension, although membrane ruffling is present, is marked with a red asterisk. In Figure S6, the calcium flux image (green) is overlaid on the DIC image, and it is seen that all cells that flux calcium show flattening and membrane extension. This is most dramatic in the cell highlighted with a yellow asterisk, with a membrane extension marked by blue arrows that began within seconds of the calcium flux and continued for several minutes thereafter. Furthermore, the two cells highlighted with white asterisks in panel 1 do not show any calcium flux and do not show development of any membrane extensions. This demonstrates that functional responses are induced by cell-to-cell contact over distance, presumably via TNT. It is clear from this result that spreading is not induced solely by microbial or inflammatory stimuli but can result from direct physical contact, independently of receptor engagement.

Intercellular Transfer of Small Molecules via TNT

To test whether molecules transferred by TNT are subject to any size restrictions, we used the classical method to assess connectivity between cells (generally via gap junctions), which is to coinject individual cells with a fluid phase marker (Lucifer yellow) and a small particulate marker such as Texas red dextran (TRD). When connectivity is limited but present, the fluid phase marker moves between cells, and the TRD remains within the cell that was microinjected. Following microinjection of a single cell in a dense field of THP-1 with a mixture of the two markers, Lucifer yellow moved between cells, but TRD stayed within the injected cell (Figure 7). In other injected cells, TRD did move to an adjacent cell (not shown) but not to multiple cells. Furthermore, the Lucifer yellow never was transferred to more than five or six surrounding cells. This is probably due to limited diffusion through TNT with a small diameter and a relatively long length. These results show that the lumen of at least some TNT are patent and suggest that soluble molecules in the cytosol, including protein or peptide antigens, might be transferred from cell to cell by this means. Lucifer yellow is only faintly

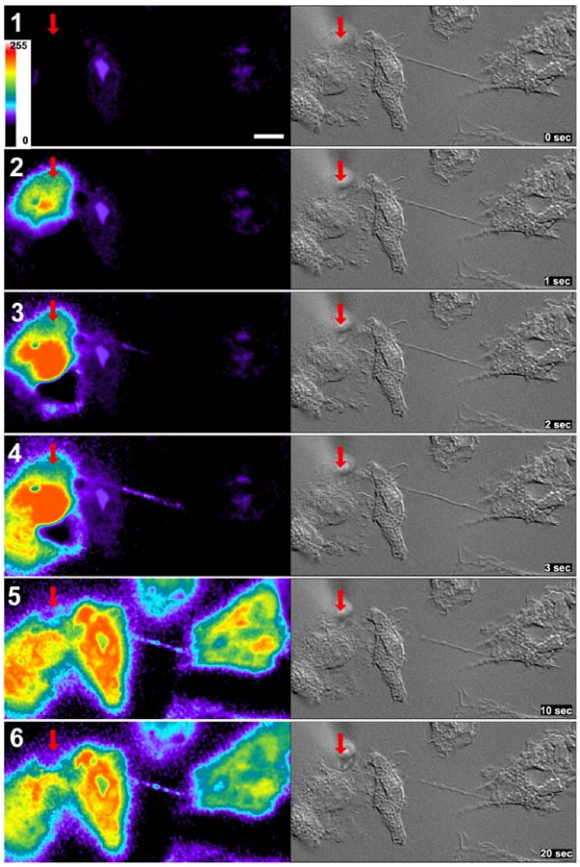

Figure 5. Calcium Flux Propagates along TNT in DC

Each panel shows a pseudocolored intensity image for the calcium signal (see [A] for intensity values) on the left and the corresponding differential interference contrast image on the right. The red arrow indicates the position of the microinjection needle used to touch the cell. This series shows DC at high magnification; a relatively large (approximately 250 nm diameter) TNT can be seen to interconnect cells in the DIC image in panel 1. Each frame (1–4) is separated by 1 s following stimulation in panel 1. The calcium flux can be clearly seen moving along the TNT connecting the cells. Panels 5 and 6 are taken at 10 and 20 s, respectively. At 10 s, significant calcium flux has occurred in all cells. In panel 5, the TNT has a beaded appearance; this is more clearly seen in panel 6 at 20 s. Scale bar equals 10 μm. Transmission of fluxes down large-diameter TNT that were similar to this data set were seen in at least five different experiments.

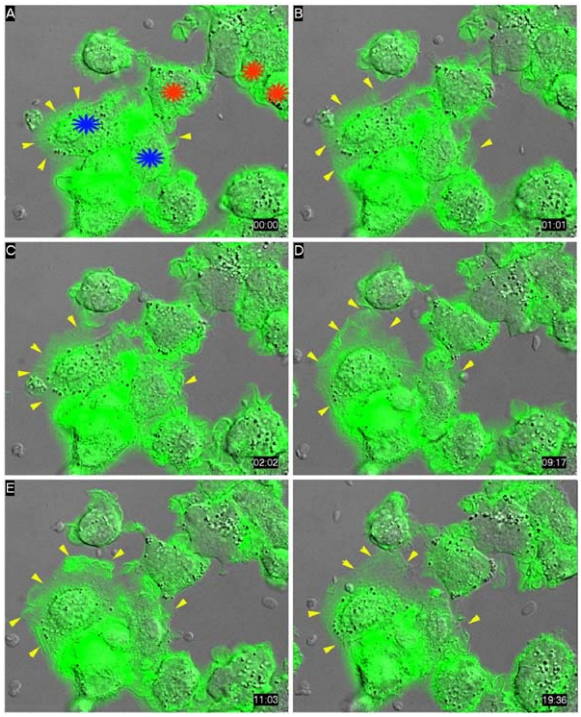

Figure 6. Calcium Flux Is Followed by Extension of Membrane Veils in DC

Allophycocyanin-labeled anti-CD11c was added to cells during the labeling with fura-2. A single cell was then mechanically stimulated and calcium fluxes observed within a larger field of cells (full field not shown). A region of the field 100 μm away from the stimulated cell is shown in the panels in this figure. All cells fluxed calcium except for the three that are marked with red asterisks. Time = 0 shown indicates 15 s after the triggering cell was stimulated and calcium fluxes had occurred. Two cells marked with blue asterisks show veil extension particularly clearly after 1 min and continuing over the time course of the experiment (20 min). The margins of the veils extended by each cell are marked with yellow arrowheads. No spreading was observed in cells that did not flux calcium. Scale bar equals 10 μm. Similar data were obtained in Figure S6 and in two additional experiments.

detectable within connecting TNT, possibly due to the small volume of the connecting tubules, which would limit detection of signal.

Discussion

In the current study, we have examined the possibility that DC and monocytic cells can be directly activated through exposure to bacterial products or physical contact. Unexpectedly, we observed that stimulation of a single cell in culture led to responses in adjacent cells. We demonstrate that attenuated membrane protrusions previously called tunneling nanotubules (TNT), membrane nanotubes, or cytonemes connect DC and other cells of myeloid origin. These structures 25–200 nm in diameter were first described in *Drosophila* (Kornberg, 1999) and more recently in vertebrate neural (Rustom et al., 2004) and immune (Galkina et al., 2001; Gupta and DeFranco, 2003; Onfelt et al., 2004) cells. We show here that signaling mechanisms triggered by contact stimulation in one cell can be propagated to numerous adjacent cells via TNT. Furthermore, cytosolic substances, potentially including antigens, might be transferred from cell to cell via larger TNT.

To our knowledge, these data represent the first report of transmission of intercellular signals by TNT in any cell type. This appears to represent a novel mechanism that is independent of gap junctions, based on lack of classical gap junction morphology and insensitivity to the gap junction inhibitors in the myeloid cells studied. Based upon the rate at which the wave is propagated (35–10 μm s^{-1}), transmission appears distinct from more rapid types of propagation such as an action potential. While electrical conductivity is mediated by

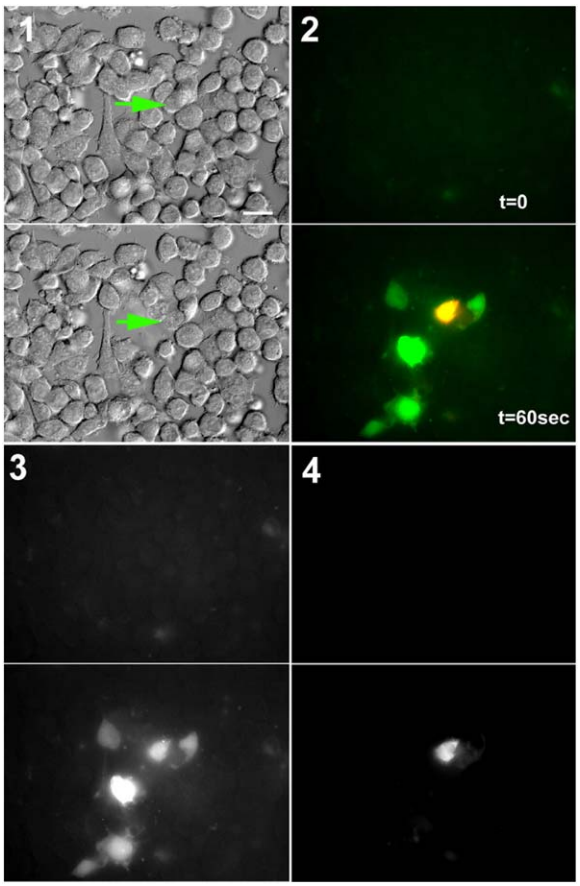

Figure 7. TNT Allow Material to Pass between Cells

A single THP-1 cell prior to (upper row) or following (lower row) injection with a mixture of Lucifer yellow and Texas red dextran is shown. Panel 1 shows the DIC image of the field of cells with the microinjected cell indicated with a green arrow immediately before injection (upper half) or 60 s after injection was completed (lower half). Panel 2 shows an overlay of the Lucifer yellow-positive cells (shown individually in panel 3) and the Texas red dextran-positive cells (shown individually in panel 4). Lucifer yellow transfers to several cells in the field, while Texas red dextran is contained within the microinjected cell. Scale bar equals 10 μm. Results are representative of five independent experiments.

gap junctions in many cell types, our results support the existence of a previously undescribed mechanism. Whether TNT-mediated connections between myeloid cells retain some features of classical gap junctions, such as involvement of connexins, must be determined.

A soluble factor from *E. coli* (ECS) can initiate the signal in a single DC that is then propagated to other myeloid cells, supporting the physiologic relevance of these observations (Figure 2). How bacterial supernatant ECS stimulates fluxes is unknown, but its potency is reduced by chloroform extraction (data not shown). The active component is unlikely to be LPS, since this only weakly stimulates a flux in DC (data not shown), and it is possible that this is due to contaminants present in the impure commercial source of LPS we have used.

Immune cells, including B cells, T cells, NK cells, neutrophils, and monocytes, have been shown recently to form TNT (Galkina et al., 2001; Gupta and DeFranco, 2003; Onfelt et al., 2004). GPI-linked GFP was able to transfer from a B cell line to other cell types, demonstrating continuity of the plasma membranes of the two cells. However, it is not known whether signaling via TNT would be relevant to activation of T lymphocytes, for example, since synapses that form between them and APC such as B cells require close opposition of membranes at an extensive interface. Furthermore, as noted previously, we have not observed propagation of calcium fluxes in nonmyeloid cells such as fibroblasts, even when TNT appear to connect cells.

It has been shown that antigen-presenting cells of the myeloid lineage can take up antigens from other cell types, and based on the current results, we suggest that this could be carried out by cells connected by TNT. In addition, signals propagated via TNT may have important roles in initiating and amplifying signals in sentinel cells such as DC that trigger immune responses. Contact of antigen or inflammatory stimuli with DC in the periphery is likely to lead to activation of other interconnected cells, generating a grouped response to exogenous stimulus. This may allow faster, more efficient processing of antigens. Activation of multiple cells that are directly connected may also lead to a local inflammatory response more rapidly than would occur if inflammation were directed solely by secretion of soluble mediators such as cytokines.

A role for TNT in vivo has not yet been demonstrated, and it should be considered whether such structures could connect cells in a dense cellular environment. In this regard, it is interesting to note that DC underlying the gut epithelial layer can project dendrites between cells that pass through tight junctions before forming balloon structures to access bacteria in the gut lumen (Niess et al., 2005). It is possible that TNT in vivo would similarly be constrained by the local cellular environment and that this would determine their function at specific sites. Interactions between migratory DC and resident DC in lymph nodes, for example, which may allow for dispersal of antigen from the former to the latter (Lindquist et al., 2004), might occur through TNT-mediated connections. DC-T cell interactions in lymph nodes, which also require encounters between large numbers of cells (Miller et al., 2004; Stoll et al., 2002), could also involve TNT. Cell interactions within lymph nodes have been best studied to date using 2-photon microscopy, which has a resolution limit above that needed to visualize TNT. Thus, further development of imaging technologies will likely be needed to fully address potential functions of TNT in vivo.

Experimental Procedures

Cells and Reagents

DC were cultured from CD14+ peripheral blood monocytes as previously described (Dong et al., 1999). Briefly, PBMC were purified by Ficoll-Pague (Amersham Pharmacia, Uppsala, Sweden) gradient centrifugation of commercially purchased buffy coats obtained from healthy blood donors. Monocytes were obtained by 1 hr adherence to plastic in Iscoves medium (IMDM, GIBCO, Rockville, MD). After washing, adherent cells were cultured in flasks for 5

days in IMDM containing 10% FCS with GM-CSF and IL-4 (1000 U/ml). THP-1 cells (obtained from Dr. Olja Finn) are a monocytic cell line that can acquire macrophage functions following treatment with compounds such as LPS or PMA. For imaging analysis, both types of cells were plated in collagen-coated chamber slides (Lab-tek, Campbell, CA). Alexa488-labeled anti-HLA-A,B,C was obtained from Serotec (Oxford, UK), and allophycocyanin-labeled anti-human CD11c was from Becton-Dickinson (San Jose, CA). All other reagents were from Sigma (St. Louis, MO) unless otherwise mentioned.

Imaging

All imaging for this study was performed using a Nikon (Melville, NY) TE 2000E equipped with a Perkin Elmer (Boston, MA) Ultraview spinning disk confocal microscope, as well as wide-field imaging capabilities and an Eppendorf micro-injection system. For both wide-field and confocal imaging, Q-Imaging Retiga EXI cameras (Burnaby, BC, Canada) were used. Excitation filter wheels were from Sutter (Novato, CA). For fura-2 measurements, all filters in the microscope were provided by Chroma (Brattleboro, VT). Metamorph (Molecular Devices, Downingtown, PA) was used to collect all data and to drive the microscope. All images were collected using a 1.3 NA oil immersion 40× objective with a 1× coupler between the microscope and either the confocal or wide-field cameras. Cells were maintained at 37°C in the microscope using a Harvard Apparatus heated stage insert (Holliston, MA). The XYZ stage used is made by ASI (Eugene, OR).

Ratiometric Experiments

Cells were loaded with FURA 2-AM by the following protocol. A stock vial of Fura 2AM (Molecular Probes, Eugene, OR) was resuspended in 50 μl of DMSO, and 10 μl of this product was diluted in 2 ml of sterile PBS (final concentration of FURA 2AM = 5 μM). Cells were washed in sterile PBS once and then incubated for 30 min in FURA 2 AM at 37°C, washed in warm media, and placed in the microscope to stabilize for 10 min. To stimulate the cells, a new, sterile, femto-tip loaded with media was placed in the microinjector under no back pressure (control experiments with tips loaded with dye showed no release, as imaged by fluorescence microscopy under these conditions). Tips were moved into close proximity (about 1 μm away) from the cells being studied and image frames collected. In each case, images were collected using excitation at 340 nm, 380 nm, and with DIC. The DIC analyzer was removed automatically following collection. Frames were collected such that all three images were collected in 1 s. Generally, images were binned 2×2 for ratiometric image collection, and exposure time was 40 ms for 340, 30 ms for 380, and 25 ms for DIC. This minimizes phototoxicity to the cells and quenching of the FURA-2. Once imaging commenced, the microinjection tip was moved slowly toward a cell such that it touched and slight deformation of the plasma membrane was seen. If any perturbation beyond slight deformation occurred, this stage position was rejected. Imaging was continued for at least another 2 min following stimulation. Generally by this time, the calcium flux had occurred and cells were seen to return to baseline or close to baseline levels. In some experiments, we stimulated a single cell to allow flux to occur across the field and then stimulated another cell that did not flux in the first stimulus. In these experiments, imaging was continued throughout the sequence of stimulations. Ratios were calculated using Metamorph and images presented as pseudocolored intensity profiles.

Confocal Microscopy

Live-cell confocal microscopy was used to image DC and THP-1 cells. Cells were labeled with Alexa Fluor 488 conjugated to antibodies to MHC class I (mouse anti-human HLA-A,B,C, Serotec) and used at 1 μg/ml by diluting the antibody into the media in the microscope. Labeling was allowed to continue for 15 min prior to imaging, at which time signal was readily detectable on the surface of DC and THP-1 cells. To collect confocal data sets, Metamorph was used to select the top and bottom positions of cells in the field and sequences collected in Z at Nyquist sampling frequency (generally 20 Z axis positions). Reconstructions were made using Metamorph.

Fixed cell confocal microscopy was performed by fixing cells in dishes in 2% paraformaldehyde for 10 min, permeabilizing in 2% paraformaldehyde containing 0.1% triton X100 (10 min) washing in PBS and then incubating in rhodamine phalloidin (2 units/ml) for 30 min. After washing in PBS, imaging was performed using an Olympus fluoview 1000 confocal microscope with a 40× 1.3NA oil immersion objective (Z projections were generated as for the live-cell imaging confocal above).

Scanning Electron Microscopy

Cells were fixed in 2% glutaraldehyde in PBS for 20 min and post-fixed in 1% osmium tetroxide for 20 min following washing in PBS. Cells were dehydrated through a graded series of alcohols, critical point dried, and coated with 3 nm gold palladium. Imaging was with a JEOL (Peabody, MA) 95335 Field emission gun SEM.

Supplemental Data

Supplemental Data include six figures and six movies and can be found with this article online at http://www.immunity.com/cgi/content/full/23/3/309/DC1/.

Acknowledgments

The authors thank Dr. Katy Baty for technical advice on microinjection and for performing control experiments with gap junction inhibitors, Mr. Stuart Shand for performing confocal microscopy, and Dr. Larry Kane and Dr. Olivera Finn for critical reading of the manuscript. This work was supported by NIH grant CA73743. The authors declare that they have no competing financial interests.

Received: May 2, 2005
Revised: July 14, 2005
Accepted: August 24, 2005
Published: September 20, 2005

References

Agrawal, S., Agrawal, A., Doughty, B., Gerwitz, A., Blenis, J., Van Dyke, T., and Pulendran, B. (2003). Cutting edge: different Toll-like receptor agonists instruct dendritic cells to induce distinct Th responses via differential modulation of extracellular signal-regulated kinase-mitogen-activated protein kinase and c-Fos. J. Immunol. *171*, 4984–4989.

Ballarin, L., Scanferla, M., Cima, F., and Sabbadin, A. (2002). Phagocyte spreading and phagocytosis in the compound ascidian *Botryllus schlosseri*: evidence for an integrin-like, RGD-dependent recognition mechanism. Dev. Comp. Immunol. *26*, 345–354.

Bambou, J.-C., Giraud, A., Menard, S., Begue, B., Rakotobe, S., Heyman, M., Taddei, F., Cerf-Bensussan, N., and Gaboriau-Routhiau, V. (2004). In vitro and ex vivo activation of the TLR5 signaling pathway in intestinal epithelial cells by a commensal *Escherichia coli* strain. J. Biol. Chem. *279*, 42984–42992.

Boitano, S., and Evans, W.H. (2000). Connexin mimetic peptides reversibly inhibit Ca^{2+} signaling through gap junctions in airway cells. Am. J. Physiol. Lung Cell. Mol. Physiol. *279*, L623–L630.

Cox, D., Berg, J.S., Cammer, M., Chinegwundoh, J.O., Dale, B.M., Cheney, R.E., and Greenberg, S. (2002). Myosin X is a downstream effector of PI(3)K during phagocytosis. Nat. Cell Biol. *4*, 469–477.

Dong, X., Storkus, W.J., and Salter, R.D. (1999). Binding and uptake of agalactosyl IgG by mannose receptor on macrophages and dendritic cells. J. Immunol. *163*, 5427–5434.

Fitzgerald, K.A., Rowe, D.C., and Golenbock, D.T. (2004). Endotoxin recognition and signal transduction by the TLR4/MD2-complex. Microbes Infect. *6*, 1361–1367.

Galkina, S.I., Sud'ina, G.F., and Ullrich, V. (2001). Inhibition of neutrophil spreading during adhesion to fibronectin reveals formation of long tubulovesicular cell extensions (cytonemes). Exp. Cell Res. *266*, 222–228.

Gupta, N., and DeFranco, A.L. (2003). Visualizing lipid raft dynamics and early signaling events during antigen receptor-mediated B-lymphocyte activation. Mol. Biol. Cell *14*, 432–444.

Kornberg, T. (1999). Pictures in cell biology. Cytonemes. Trends Cell Biol. *9*, 434.

Lindquist, R.L., Shakhar, G., Dudziak, D., Wardemann, H., Eisenreich, T., Dustin, M.L., and Nussenzweig, M.C. (2004). Visualizing dendritic cell networks in vivo. Nat. Immunol. *5*, 1243–1250.

Miller, M.J., Safrina, O., Parker, I., and Cahalan, M.D. (2004). Imaging the single cell dynamics of CD^{4+} T cell activation by dendritic cells in lymph nodes. J. Exp. Med. *200*, 847–856.

Neijssen, J., Herberts, C., Drijfhout, J.W., Reits, E., Janssen, L., and Neefjes, J. (2005). Cross-presentation by intercellular peptide transfer through gap junctions. Nature *434*, 83–88.

Niess, J.H., Brand, S., Gu, X., Landsman, L., Jung, S., McCormick, B.A., Vyas, J.M., Boes, M., Ploegh, H.L., Fox, J.G., et al. (2005). CX3CR1-mediated dendritic cell access to the intestinal lumen and bacterial clearance. Science *307*, 254–258.

Onfelt, B., Nedvetzki, S., Yanagi, K., and Davis, D.M. (2004). Cutting edge: membrane nanotubes connect immune cells. J. Immunol. *173*, 1511–1513.

Osipchuk, Y., and Cahalan, M. (1992). Cell-to-cell spread of calcium signals mediated by ATP receptors in mast cells. Nature *359*, 241–244.

Park, J.S., Svetkauskaite, D., He, Q., Kim, J.-Y., Strassheim, D., Ishizaka, A., and Abraham, E. (2004). Involvement of Toll-like receptors 2 and 4 in cellular activation by high mobility group Box 1 protein. J. Biol. Chem. *279*, 7370–7377.

Pasare, C., and Medzhitov, R. (2004). Toll-like receptors: linking innate and adaptive immunity. Microbes Infect. *6*, 1382–1387.

Rustom, A., Saffrich, R., Markovic, I., Walther, P., and Gerdes, H.-H. (2004). Nanotubular highways for intercellular organelle transport. Science *303*, 1007–1010.

Salter, R.D., Tuma-Warrino, R.J., Hu, P.Q., and Watkins, S.C. (2004). Rapid and extensive membrane reorganization by dendritic cells following exposure to bacteria revealed by high-resolution imaging. J. Leukoc. Biol. *75*, 240–243.

Stoll, S., Delon, J., Brotz, T.M., and Germain, R.N. (2002). Dynamic imaging of T cell-dendritic cell interactions in lymph nodes. Science *296*, 1873–1876.

Takeda, K., and Akira, S. (2004). TLR signaling pathways. Semin. Immunol. *16*, 3–9.

Wells, C.M., Walmsley, M., Ooi, S., Tybulewicz, V., and Ridley, A.J. (2004). Rac1-deficient macrophages exhibit defects in cell spreading and membrane ruffling but not migration. J. Cell Sci. *117*, 1259–1268.

West, M.A., Wallin, R.P.A., Matthews, S.P., Svensson, H.G., Zaru, R., Ljunggren, H.-G., Prescott, A.R., and Watts, C. (2004). Enhanced dendritic cell antigen capture via Toll-like receptor-induced actin remodeling. Science *305*, 1153–1157.